

DOI: 10.1002/cmdc.200600118

## Activatable Fluorescent Probes for Tumour-Targeting Imaging in Live Mice

Jesus Razkin,<sup>[a]</sup> Véronique Josserand,<sup>[d]</sup>  
Didier Boturyn,<sup>\*[a]</sup> Zhao-hui Jin,<sup>[c]</sup> Pascal Dumy,<sup>\*[a]</sup>  
Marie Favrot,<sup>[c]</sup> Jean-Luc Coll,<sup>[c]</sup> and Isabelle Texier<sup>\*[b]</sup>

The direct and noninvasive in vivo visualisation of molecular processes such as ligand–receptor interaction, enzymatic activity, or gene expression, is the goal of molecular imaging.<sup>[1,2]</sup> Optical imaging appears as a new complementary modality to the traditional nuclear or MRI (magnetic resonance imaging) techniques because of its low cost and fewer constraints.<sup>[3,4]</sup> Thus, the need for new optical probes with increased targeting and imaging capabilities arises.<sup>[5,6]</sup> Tung et al. introduced the concept of “smart” or activatable probes for imaging the activity of proteases over-expressed in mice tumours, such as MMP2 or cathepsin D.<sup>[7–9]</sup> In these activatable probes, Cy5.5 dyes are grafted to peptide branching arms of a co-polymer, in such a way that they auto-quench initially. Whenever the proteases specifically cut the peptide sequence, the Cy5.5 fluorescence is recovered.<sup>[7–11]</sup>

In the present work, the concept of activatable probes is extended to the imaging of different molecular events, in the expectation of improving the image contrast in comparison to that obtained with classical targeting agents.<sup>[12]</sup> The molecular structures we propose can be used for imaging enzymatic activity, specific targeting, and molecular processes triggered by ligand–receptor interaction. Moreover, their nonpolymeric nature can be very well controlled and characterised for pharmacology and medical applications. These activatable probes are built on a cyclodecapeptide template named RAFT (Regionally Selectively Addressable Functionalized Template),<sup>[13]</sup> a new molecular vector for targeted drug delivery and molecular imaging of tumours and metastasis.<sup>[14]</sup> This new class of molecules differs from other systems by the topological separation of two independent functional domains, which can be addressed

in a spatially controlled manner: a cell targeting domain, and a therapeutic or imaging domain (Scheme 1).<sup>[14,15]</sup> Clustered RGD-containing markers are used for cell recognition by the  $\alpha_v\beta_3$  integrin,<sup>[16–19]</sup> a vitronectin receptor over-expressed on the surface of endothelial cells of growing blood vessels, and therefore a cardinal feature of many malignant tumours.<sup>[19–21]</sup> A multimeric presentation of the RGD motif is essential for integrin-mediated internalisation of the probe.<sup>[16,17,22–24]</sup>

In the activatable probes we designed, the imaging function is composed of the cyanine 5 fluorescent dye (Cy5), a cleavable bond, and a quencher (Q). The cleavable bond is used to follow the cellular internalisation of the probe induced by binding to its receptor. Disulfide bridges are known to be reduced enzymatically by thioredoxines in the cytosol,<sup>[25,26]</sup> and have been used to improve the efficiency of targeted drug delivery.<sup>[26–29]</sup> The redox potential within the endosomal system could also be reducing.<sup>[25–29]</sup> Therefore, -Cysteine-S–S–Cysteine- (abbreviated as S–S below) is chosen as a cleavable bond, to follow the internalisation of the fluorescent probe into the cells after its RGD-mediated binding on their surface. Demonstrating targeting can be crucial for screening and comparing the recognition efficiency of different biological markers. Moreover, demonstrating internalisation is also very important to estimate the ability of a molecule, such as the RAFT, to be used as a vector for targeted drug delivery.

The self-quenching of the cyanine dyes allows the use of the Cy5-S–S-Cy5 group as an activatable unit (Scheme 1).<sup>[30]</sup> Alternatively, a diaryl rhodamine derivative quencher (QSY21) can be used in place of one of the Cy5 units.<sup>[31]</sup> Cy5 fluorescence is markedly inhibited in the Cy5-S–S-QSY21 group (Table 1). This dynamic and static quenching<sup>[32]</sup> in aqueous buffer can be accounted for by the hydrophobic nature and opposite charges of the molecules, which favour their stacking. In this context, the RAFT-(cRGD)<sub>4</sub>-Cy5-S–S-Cy5 **1**, RAFT-(cRGD)<sub>4</sub>-Cy5-S–S-QSY21 **2**, and RAFT-(cRGD)<sub>4</sub>-QSY21-S–S-Cy5 **3** have been synthesised (Scheme 1). The peptide moiety of the molecule is prepared by a combination of solid and solution phase synthesis using a Fmoc/tBu strategy, followed by a chemoselective assembling of ligand moieties and template, as reported elsewhere.<sup>[14,15]</sup> Npys-protected cysteine is chosen to graft the fluorescent unit to the RAFT. This allows a regioselective disulfide bond formation. Cy5 and QSY21, available in the activated ester form, are then attached successively to the macromolecule, providing, after RP-HPLC purification, the desired compounds in satisfying overall yields (13–18%).

The activation of the fluorescent probes is demonstrated first in vitro. Figure 1A displays the absorption spectra of the RAFT-(cRGD)<sub>4</sub>-Cy5-S–S-QSY21 **2** before and 2 h after addition of 2-mercaptoethanol (2-MCE). The spectrum after cleavage matches that of the sum of Cy5 and QSY21, whereas for **2**, the electronic interaction between the dye and quencher is evidenced by an intense absorption band at 600 nm. Similar results are obtained for **1**: the 600 nm absorption band in this case is indicative of the presence of Cy5 dimers, whereas the 647 nm band is attributed to the dye monomer.<sup>[30]</sup> Fluorescence measurements (Figure 1B) show the initial Cy5 fluorescence quenching and its 100% recovery upon the S–S bond

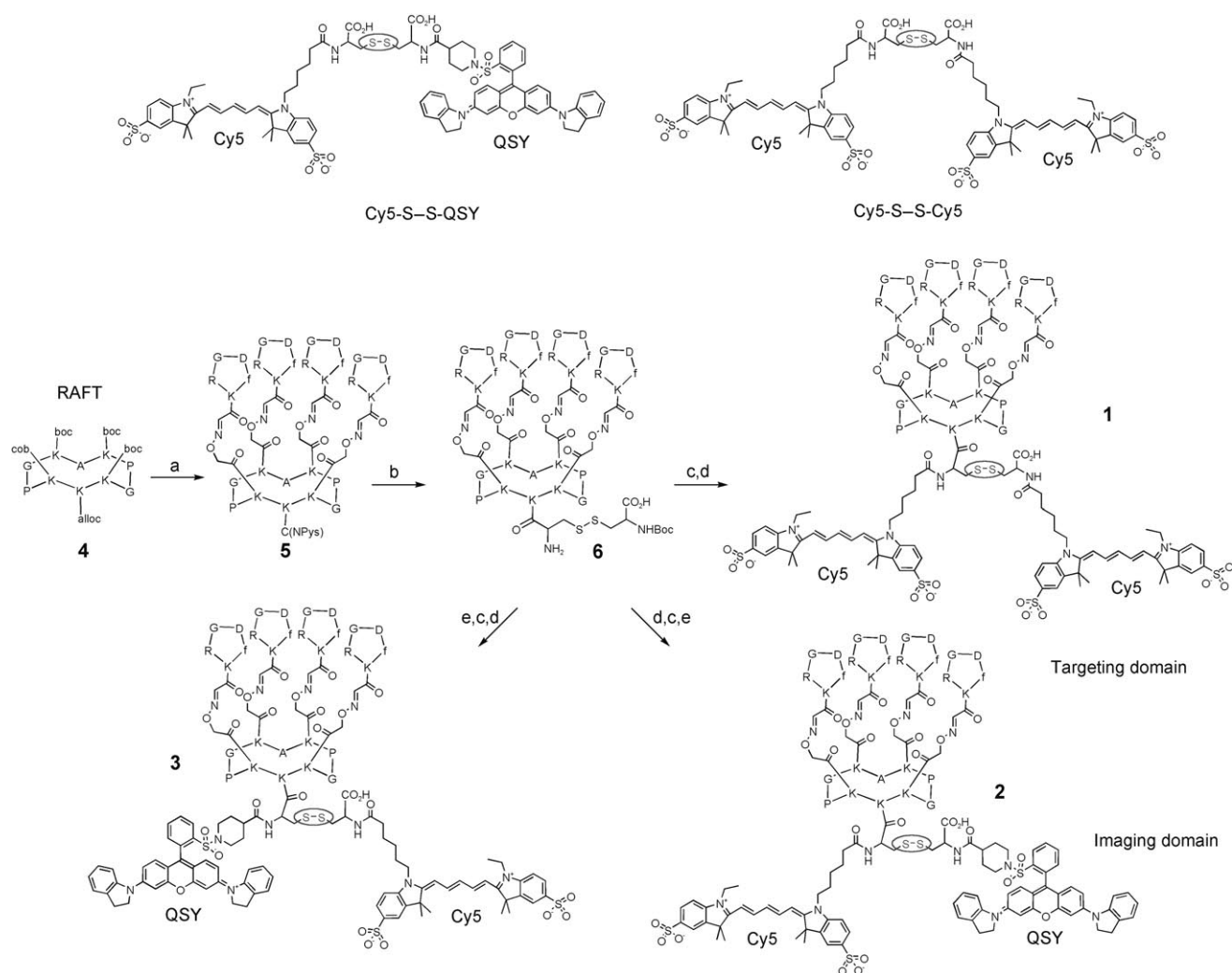
[a] Dr. J. Razkin, Dr. D. Boturyn, Prof. P. Dumy  
LEDSS, UMR CNRS 5616, 301 rue de la chimie, BP 53,  
38041 Grenoble Cedex 9 (France)  
Fax: (+33)476-635-540  
E-mail: Didier.Boturyn@ujf-grenoble.fr

[b] Dr. I. Texier  
LETI/DTBS CEA Grenoble, 17 rue des martyrs,  
38054 Grenoble Cedex 9 (France)  
Fax: (+33)438-785-787  
E-mail: isabelle.texier-nogues@cea.fr

[c] Dr. Z.-h. Jin, Prof. M. Favrot, Dr. J.-L. Coll  
INSERM U578, Institut Albert Bonniot, 38706 La Tronche (France)

[d] Dr. V. Josserand  
ANIMAGE—CREATIS, Bâtiment CERMEP, 59 Boulevard Pinel,  
69677 Bron Cedex (France)

Supporting information for this article is available on the WWW under <http://www.chemmedchem.org> or from the author.



**Scheme 1.** Structure and synthesis scheme of the fluorescent probes. Reagents: a) 1. TFA/DCM (1:1); 2. BocNHCH<sub>2</sub>CONHS, DMF; 3. Pd(PPh<sub>3</sub>)<sub>4</sub>, PhSiH<sub>3</sub>, DCM; 4. BocC(Npys), PyBOP, DMF, 5. TFA, TIS H<sub>2</sub>O (90:5:5); 6. H<sub>2</sub>O/CH<sub>3</sub>CN (1:1), c[RGDFK(COCHO)-]. b) BocCys, DMF/PBS (3:1). c) TFA/DCM (1:1). d) Cy5NHS, DIEA, DMF. e) QSYNHS, DIEA, DMF.

**Table 1.** Photophysical properties of the probes, and the in vitro rates of the disulfide bonds cleavage.<sup>[a]</sup>

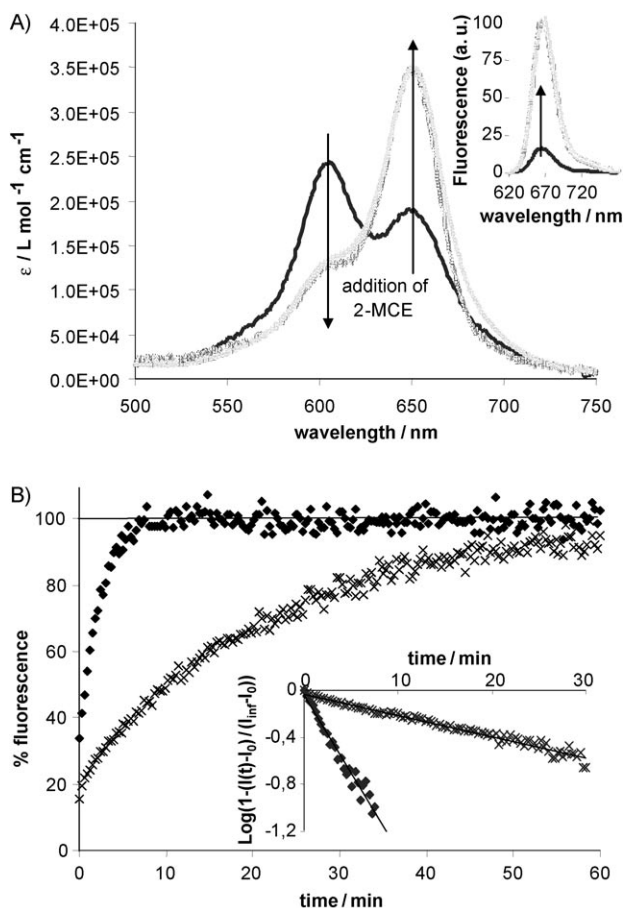
Molecules	$\lambda_{\text{exc}}$ [nm] ( $\epsilon$ [L mol <sup>-1</sup> cm <sup>-1</sup> ]) <sup>[b]</sup>	$\lambda_{\text{em}}$ [nm] <sup>[c]</sup>	$\Phi/\Phi(\text{Cy5})$ <sup>[d]</sup>	Cleavage rate [min] <sup>[e]</sup>
Cy5	600 ( $0.7 \times 10^5$ ), 648 ( $2.5 \times 10^5$ )	664	100 %	-
Cy5-S-S-Cy5	603 ( $3.0 \times 10^5$ ), 642 ( $2.0 \times 10^5$ )	663	( $5.5 \pm 0.5$ ) % <sup>[f]</sup>	$31 \pm 5$
1	604 ( $2.6 \times 10^5$ ), 646 ( $3.0 \times 10^5$ )	667	( $23 \pm 1$ ) % <sup>[f]</sup>	$7.6 \pm 1.2$
Cy5-S-S-QSY21	603 ( $2.8 \times 10^5$ ), 642 ( $1.6 \times 10^5$ )	664	( $0.5 \pm 0.1$ ) %	$5.3 \pm 1.1$
2	604 ( $2.5 \times 10^5$ ), 649 ( $1.9 \times 10^5$ )	664	( $16 \pm 1$ ) %	$55 \pm 9$
3	602 ( $1.8 \times 10^5$ ), 647 ( $1.6 \times 10^5$ )	665	( $16 \pm 1$ ) %	$5.9 \pm 0.8$

[a] Probes  $\approx 1 \mu\text{M}$  in PBS 10 mM, pH 7.4. [b] Absorption wavelengths ( $\pm 1$  nm) and extinction coefficients ( $\pm 0.1 \times 10^5$ ). [c] Emission wavelength ( $\pm 1$  nm, excitation at 600 nm). [d] Relative fluorescence quantum yield (excitation at 600 nm). [e] First-order time constants for fluorescence recovery recorded at 665 nm, upon addition of 85 mM of 2-MCE (excitation at the isobestic point at 622 nm). The data were fitted with  $R^2 > 0.98$ . [f] % of the fluorescence of 2Cy5 molecules.

cleavage. As summarised in Table 1, the fluorescence quantum yields and the rates of the cleavage of the disulfide bridge are greatly affected by the nature and the spatial localisation of the different units on the RAFT template.

Probe cellular internalisation is evidenced by confocal microscopic observation using HEK293( $\beta_3$ ) cells overexpressing  $\alpha_v\beta_3$

integrin.<sup>[22]</sup> Specific cellular uptake of the quenched probe RAFT-(cRGD)<sub>4</sub>-Cy5-S-S-Cy5 is supported by the negative staining with the control probe RAFT-(cRAD)<sub>4</sub>-Cy5 (Figure 2A). The quenched probe produces weaker staining of the cell membrane than RAFT-(cRGD)<sub>4</sub>-Cy5, which is probably a result of its quenched Cy5 emission (Figure 2A). The intracellular signal



from the quenched probe also appears with a higher contrast, suggesting site-limited fluorescence activation (Figure 2A). The colocalisation of RAFT-(cRGD)<sub>4</sub>-Cy5-S-S-Cy5 and a lysosome-labelling dye suggests this cellular compartment as the possible cleavage location of the disulfide bond (Figure 2B).

Before injection in mice, the chemical stability of the probes is checked in blood samples. No fluorescence increase is observed upon incubation at 37 °C of 1 μM of the activatable Cy5-S-S-Q, in plasma or whole blood, for at least 120 min. In a preliminary experiment, the RAFT activatable probes 1 and 2 were injected intravenously (IV) into a tumour bearing mouse (one per group) and followed noninvasively by whole body fluorescence imaging (Figure 3).<sup>[33]</sup> The human ovarian cancer cell line IGROV1 is used as a tumour model because of its expression of α<sub>v</sub>β<sub>3</sub> integrin.<sup>[22]</sup> In these mice, the use of the activatable probes dramatically increases the image contrast in comparison to the previously described RAFT-(cRGD)<sub>4</sub>-Cy5 molecule.<sup>[34]</sup> Indeed, a few minutes after IV injection, the unquenched probe accumulates in the tumour, but the presence of unbound circulating molecules in normal tissues greatly reduces the tumour:background ratio (contrast). We observed that the Cy5 fluorescence recovery of the activatable probes is

**Figure 1.** A) Absorption and emission spectra, RAFT-(cRGD)<sub>4</sub>-Cy5-S-S-QSY21: black; RAFT-(cRGD)<sub>4</sub>-Cy5-S-S-QSY21 2 h after 2-MCE addition: dark grey; Cy5 + QSY21: light grey, and B) Cy5 fluorescence recovery, (insert: fit by pseudo-first order kinetics) upon cleavage of the disulfide bond by 2-MCE. (1 μM probes, 70 mM 2-MCE, in PBS 10 mM, pH 7.4), RAFT-(cRGD)<sub>4</sub>-Cy5-S-S-QSY21: ♦; RAFT-(cRGD)<sub>4</sub>-Cy5-S-S-QSY21: ×.

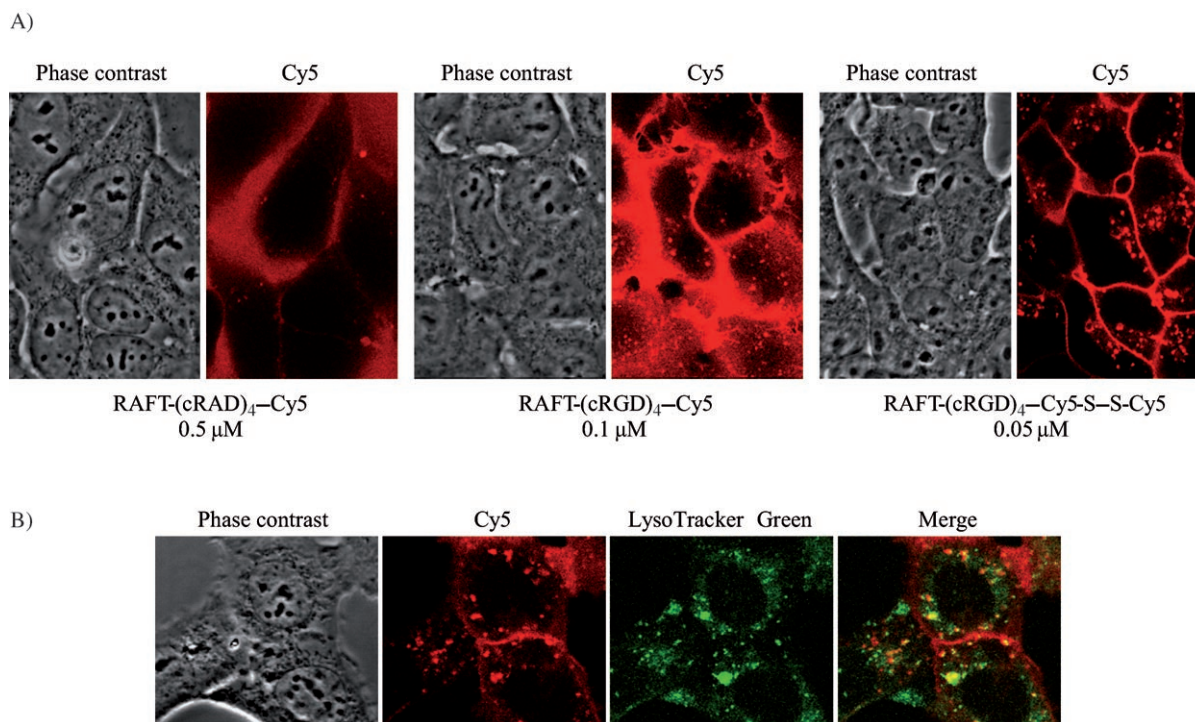


**Figure 2.** Confocal microscopic images of cellular uptake and activation of RAFT-(cRGD)<sub>4</sub>-Cy5-S-S-Cy5 1 (0.05 μM) in live HEK293(β<sub>3</sub>) cells after 1.5 h incubation at 37 °C. A) Phase contrast and Cy5 fluorescence (pseudo-coloured red) images. B) Colocalisation of Cy5 (pseudo-coloured red, 635 nm excitation) and a lysosome-labeling probe, LysoTracker Green (0.05 μM, pseudo-coloured green, 488 nm excitation).



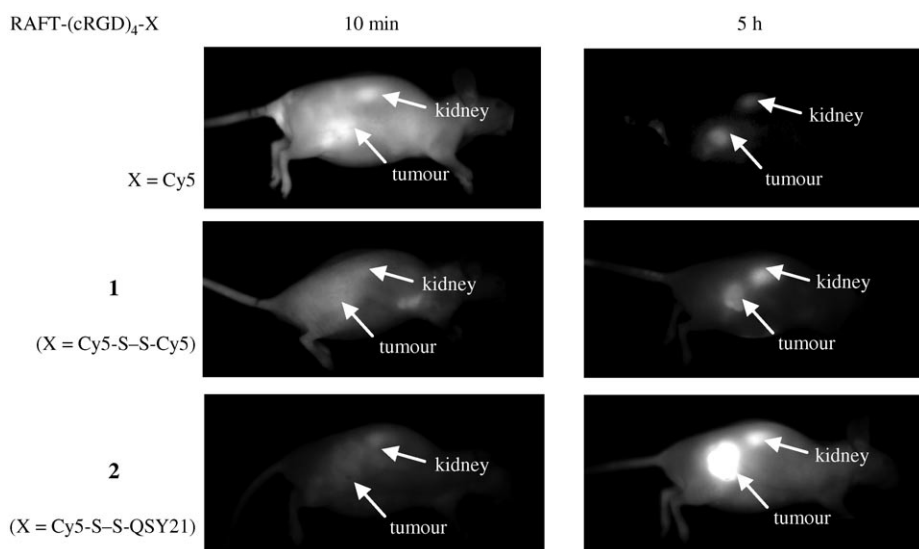


**Figure 3.** Fluorescence imaging of subcutaneous IGROV1 tumour-bearing mice, 10 min and 5 h after IV injection of the probes (dissolved in PBS 10 mM, pH 7.4, with 10% DMSO, 10% EtOH), at 10 nmol Cy5 per mouse. The images are acquired and presented with the same camera settings, with the fluorescence ranging from 1811 to 42429 photons per pixel.

slow, and 5 h after the IV injection the contrast is greatly augmented (Figure 3). These preliminary results have been confirmed using a greater number of mice per group, and will be detailed in a dedicated publication, including pharmacokinetic characterisation.

In conclusion, new fluorescent probes for tumour imaging in mice are developed, based on a nonpolymeric and well-characterised peptide scaffold.<sup>[14]</sup> Specific activation of the fluorescence may have the potential for improving image contrast. Thanks to the easily triggered dequenching of dye fluorescence, optical probes can be easily designed for functional imaging. Therefore, we can envision that the optical imaging techniques will be complementary to other modalities (PET, MRI, CT), and will open new possibilities for in vivo molecular imaging.

## Acknowledgements

This work was supported by the Association pour la Recherche contre le Cancer (ARC N° 3741), the Ministère de la Recherche (ACI N° 02L0525), the Région Rhône-Alpes (N° 0301372501 and 0301372502), the Cancéropôle (N° 032115 and 042259), the Université Joseph Fourier, the Centre National de la Recherche Scientifique (CNRS), the Institut National de la Santé Et de la Recherche Médicale (INSERM) and the Commissariat à l'Energie Atomique (CEA).

**Keywords:** fluorescent probes · imaging agents · molecular recognition · peptide scaffold

- [1] T. F. Massoud, S. S. Gambhir, *Genes Dev.* **2003**, *17*, 545.  
 [2] F. A. Jaffer, R. Weissleder, *J. Am. Med. Assoc.* **2005**, *293*, 855.  
 [3] V. Ntziachristos, J. Ripoll, L. V. Wang, R. Weissleder, *Nat. Biotechnol.* **2005**, *23*, 313.

- [4] A. H. Hielscher, *Curr. Opin. Biotechnol.* **2005**, *16*, 79.  
 [5] C.-H. Tung, *Biopolymers* **2004**, *76*, 391.  
 [6] K. Licha, C. Olbrich, *Adv. Drug Delivery Rev.* **2005**, *57*, 1087.  
 [7] C. Bremer, C.-H. Tung, R. Weissleder, *Nat. Med.* **2001**, *7*, 743.  
 [8] C.-H. Tung, U. Mahmood, S. Bredow, R. Weissleder, *Cancer Res.* **2000**, *60*, 4953.  
 [9] R. Weissleder, C.-H. Tung, U. Mahmood, A. Bogdanov, Jr., *Nat. Biotechnol.* **1999**, *17*, 375.  
 [10] K. Kim, M. Lee, H. Park, J.-H. Kim, S. Kim, H. Chung, K. Choi, I.-S. Kim, B. Seong, I. Kwon, *J. Am. Chem. Soc.* **2006**, *128*, 3490.  
 [11] A. K. Galande, R. Weissleder, C. H. Tung, *Bioconjugate Chem.* **2006**, *17*, 255.  
 [12] S. Achilefu, *Technol. Cancer Res. Treat.* **2004**, *3*, 393.  
 [13] P. Dumy, I. M. Eggleston, S. Cervigni, U. Sila, X. Sun, M. Mutter, *Tetrahedron Lett.* **1995**, *36*, 1255.  
 [14] D. Boturyn, J. L. Coll, E. Garanger, M. Favrot, P. Dumy, *J. Am. Chem. Soc.* **2004**, *126*, 5730.  
 [15] E. Garanger, D. Boturyn, O. Renaudet, E. Defrancq, P. Dumy, *J. Org. Chem.* **2006**, *71*, 2402.  
 [16] V. Marchi-Artzner, B. Lorz, C. Gosse, L. Jullien, R. Merkel, H. Kessler, E. Sackmann, *Langmuir* **2003**, *19*, 835.  
 [17] B. Hu, D. Finsinger, K. Peter, Z. Guttenberg, M. Bärmann, H. Kessler, A. Escherich, L. Moroder, J. Böhm, W. Baumeister, S. Sui, E. Sackmann, *Biochemistry* **2000**, *39*, 12284.  
 [18] R. Haubner, R. Gratias, B. Diefenbach, S. Goodman, A. Jonczyk, H. Kessler, *J. Am. Chem. Soc.* **1996**, *118*, 7461.  
 [19] R. Haubner, D. Finsinger, H. Kessler, *Angew. Chem.* **1997**, *109*, 1440; *Angew. Chem. Int. Ed. Engl.* **1997**, *36*, 1374.  
 [20] A. Giannis, F. Rübsam, *Angew. Chem.* **1997**, *109*, 606; *Angew. Chem. Int. Ed. Engl.* **1997**, *36*, 588.  
 [21] P. Brooks, R. Clark, D. Cheresch, *Science* **1994**, *264*, 569.  
 [22] E. Garanger, D. Boturyn, Z. Jin, P. Dumy, M. Favrot, J. L. Coll, *Mol. Ther.* **2005**, *12*, 1168.  
 [23] Z. Cheng, Y. Wu, Z. Xiong, S. S. Gambhir, X. Chen, *Bioconjugate Chem.* **2005**, *16*, 1433.  
 [24] Y. Ye, S. Bloch, B. Xu, S. Achilefu, *J. Med. Chem.* **2006**, *49*, 2268.  
 [25] B. Arunachalam, U. Phan, H. J. Geuze, P. Cresswell, *Proc. Natl. Acad. Sci. USA* **2000**, *97*, 745.  
 [26] T. Maeda, K. Fujimoto, *Colloids Surf. B* **2006**, *49*, 15.  
 [27] E. P. Feener, W. C. Shen, H. J. -P. Ryser, *J. Biol. Chem.* **1990**, *265*, 18780.  
 [28] M. D. Henry, S. Wen, M. D. Silva, S. Chandra, M. Milton, P. J. Worland, *Cancer Res.* **2004**, *64*, 7995.  
 [29] C. D. Austin, X. Wen, L. Gazzard, C. Nelson, R. Scheller, S. J. Scales, *Proc. Natl. Acad. Sci. USA* **2005**, *102*, 17987.  
 [30] V. Metelev, R. Weissleder, A. Bogdanov, *Bioconjugate Chem.* **2004**, *15*, 1481.  
 [31] We measured a Stern–Volmer quenching constant of  $1.39 \times 10^5 \text{ M}^{-1}$  in PBS solution.  
 [32] M. K. Johansson, R. M. Cook, *Chem. Eur. J.* **2003**, *9*, 3466.  
 [33] I. Texier, V. Josserand, E. Garanger, J. Razkin, Z. Jin, P. Dumy, M. Favrot, D. Boturyn, J.-L. Coll, *Proc. SPIE-Int. Soc. Opt. Eng.* **2005**, *5704*, 16.  
 [34] Z. H. Jin, V. Josserand, J. Razkin, E. Garanger, D. Boturyn, M. Favrot, P. Dumy, J.-L. Coll, *Mol. Imaging* **2006**, in press.

Received: May 12, 2006

Revised: June 6, 2006

Published online on August 31, 2006